Original Article

The Potential Protective Effect of Chitosan coated Ginger Nanoparticles versus Ginger Extract Against Vancomycin-induced Renal cortex toxicity in Rats: Histological and Immunohistochemical Study

Enas Refaat, Ereny Fekry, Sally S. Mohammed and Lamiaa Mohamed Farghaly

Department of Histology and Cell Biology, Faculty of Medicine, Suez Canal University, Egypt

ABSTRACT

Introduction and Aim: Vancomycin is the first-line antibiotic in treatment of many infections. Its nephrotoxicity is the most common side effect. Some antioxidants were reported to overcome such toxicity. Ginger was recorded to be one of such agents, moreover, Ginger Nanoparticles were found to have a better absorption and distribution especially when carried on nanocarrier. Therefore, this study was designed to compare the potential protective effects of Chitosan coated Ginger Nanoparticles and Ginger against Vancomycin-induced renal cortex toxicity in rats.

Material and Methods: 60 healthy adult male albino rats were randomized into six groups, ten animals each. Group I (Control), Group II (received intragastric Ginger extract), Group III (received intragastric Chitosan coated Ginger Nanoparticles), Group IV (received I.P injection of Vancomycin), Group V (received I.P injection of Vancomycin and intragastric Ginger extract), Group VI (received Vancomycin and intragastric Chitosan coated Ginger Nanoparticles). After 7 days, animals were sacrificed, kidneys were extracted and specimens were processed for histological technique and evaluation of the mean histological score; immunohistochemical techniques and evaluation of mean optical density of immunoreactions.

Results: Group IV revealed that 80% of animals had severe histopathological changes in the proximal convoluted tubules with statistically significant increase in the mean histological score, compared to control group. There was necrosis and desquamation of their cells. Some tubular lumens were dilated while others were obstructed by casts from desquamated cells. There was statistically significant increase in the mean optical density of Anti-Caspase 3 and Anti-iNOS immunostainning, compared to control group. Group V had significant decrease in the mean histological score compared to Group IV, but, was significantly increased compared to control. Group VI revealed significant decrease in that score, compared to both Group IV and Group VI.

Conclusion: Chitosan coated Ginger Nanoparticles and Ginger extract improved vancomycin-induced renal cortex toxicity. However, Ginger Nanoparticles showed better results.

Received: 21 July 2021, **Accepted:** 20 November 2021

Key Words: Chitosan, ginger, ginger nanoparticles, Immunostaining, vancomycin nephrotoxicity.

Corresponding Author: Sally Salem Mohammed, PhD, Department of Histology and Cell Biology, Faculty of Medicine, Suez Canal University, Egypt, **Tel.**: +20 12 8418 8788, **E-mail:** sallysalem@med.suez.edu.eg

ISSN: 1110-0559, Vol. 46, No. 2

INTRODUCTION

Vancomycin (VCM) is a glycopeptide antibiotic which acts through inhibition of cell wall synthesis. It has broadspectrum bactericidal activity against multiple gram-positive bacteria especially resistant to other types of antibiotics[1,2]. However, VCM was reported to cause neutropenia, ototoxicity and nephrotoxicity[3].

VCM-induced nephrotoxicity was reported to occur through oxidative phosphorylation[4,5]. It is excreted primarily through glomerular filtration and active proximal tubular secretion. Accordingly, the proximal renal tubules are mainly affected resulting in renal tubular ischemia. VCM also interferes with the process of proximal tubules reabsorption and lead to alteration of their mitochondrial function[6].

Many studies investigated the protective effects of many antioxidants against vancomycin-induced nephrotoxicity[7,8,9].

Ginger powder is one of the most effective antioxidant, anti-inflammatory and anti-carcinogenic herbal products[10]. It was reported to produce significant increase in the levels of antioxidant enzymes and a decrease in lipid peroxidation and protein oxidation in renal tissue[11].

Nanotechnology was reported to be widely used in the medical field. Nanoparticles (NP) are tiny particles having a size ranging from 1 to 100 nm with different properties and shape. Thus, the nanoparticles can circulate the whole body and enter the cells delivering drugs into the targeted tissues[12]. The use of natural-derived NP was reported to be safe and cost-effective. Ginger-derived nanoparticles (GNPs) were found to modulate the apoptotic activity of carcinogenic agents through elevation of antioxidant enzymes. They also decrease the inflammatory cytokines and promote the healing process in inflammatory bowel disease and colitis-associated cancer[1,13].

 DOI: 10.21608/ejh.2021.82886.1531

Herbal products have some medical problems, as they have low bioavailability, are water-insoluble and need a frequent administration or even increasing dose to achieve the desired therapeutic effect. So nanocarriers, which are also nanoparticles, are now used to deliver herbal medicine into target sites by a method called novel drug delivery systems[14,15].

The nanocarriers have a long-term circulation period and a little lymphatic drainage causing a sustained drug release and concentration. Additionally, nanocarriers agents escape degradation by chemical reactions or by the mononuclear phagocytic system. Moreover, the physiochemical properties of nanocarriers enable them to have a good stability and solubility with low toxicity[14,16]. One of the recorded nanocarriers is Chitosan. It is a polysaccharide which is a favorable pharmaceutical material due to its biocompatibility and biodegradability, forming ideal hydrophilic carrier system[17].

Limited histological studies were conducted to investigate the protective role of ginger against VCM-induced nephrotoxicity compared with GNPs. Hence, the present work was designed to study and compare the potential protective effects of Chitosan coated GNPs (CGNPs) versus ginger against VCM-induced renal cortex toxicity, using histological and immunohistochemical techniques.

MATERIALS AND METHODS

Preparations

- Vancomycin was purchased from the pharmacy in the form of powder, PHARCO pharmaceuticals. Each 1 gm was diluted in 20ml of sterile water and given in a dose of 200 mg/kg[18].
- Ginger extract preparation: Ginger or Zingiber officinale is a popular spice. It contains 50–70% carbohydrates, 3–8% lipids and phenolic compounds. The phenolic compounds include gingerol, paradols, and shogaol. These gingerols and shogaol are the active ingredients of Ginger[19].

The gingerrhizomes was obtained from Abu-Auf Company. For preparation of its aqueous extract, they were washed several times with distilled water and left to dry by air. Then they were ground by a mixer forming a fine powder and stored in sterilized containers. 125 gm of ginger powder was dissolved in 1000 mL of distilled water for 12 h, at room temperature, and then filtered to obtain a final concentration of 24 mg/ml. It was stored at 4°c for use[20,21].

- Chitosan coated Ginger Nanoparticles (CGNPs) preparation: Chitosan nanoparticles were obtained from Nanogate center (Abbas El Akkad, Nasr city, 11765, Cairo, Egypt) and prepared according to the ionotropic gelation process. This technique produces nanoparticles through electrostatic interactions between two ionic agents. One of them has to be a polymer[22].

Blank nanoparticles were obtained upon the addition of a tripolyphosphate (TPP, negative charged phosphate group) solution to a Chitosan solution (polymer, positive charged)[22]. The following steps were used for preparing different solutions:

1. Preparation of Chitosan solution (concentrations of 1% was obtained)
    - 1gm of Chitosan powder (nanocarrier) was dissolved in 200ml 1% acetic acid at a neutral pH[4]
    - The mixture was slowly stirred for 6hr to obtain a homogenous transparent solution.
2. Preparation of Chitosan coated Ginger nanocarriers
    - The previously prepared aqueous Ginger extract was dissolved in Chitosan solution.
    - 150 ml of TPP was slowly added into the solution (a dropwise manner) under magnetic stirring for 20 min.
    - The clear solution turned to a turbid one indicating formation of CGNPs.

The CGNPs were separated by centrifugation at speed of 20,000 g at temperature of 4◦C for 30 min. Finally, Ginger encapsulated with Chitosan was obtained.

3. Characterization of CGNPs

A structural characterization of nano-materials was performed by Nanogate center, using JEOL JEM-2100 high resolution transmission electron microscope at an accelerating voltage of 200 kV (Figure 1).

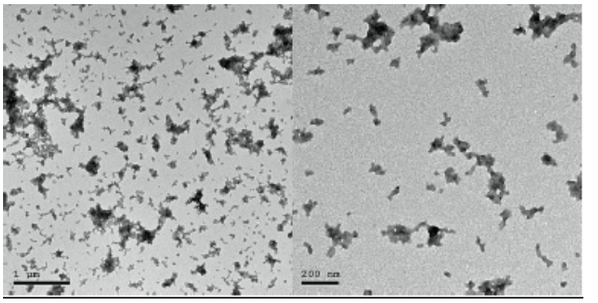

Fig. 1: Transmission electron microscopy image of the obtained Chitosan coated Ginger Nanoparticles. It showed uniform size and spherical appearance of CGNPs

Primary Antibodies

Anti-caspase3 Mouse Monoclonal (30246) was purchased from GeneTex company, North America.

Anti-iNOS rabbit Polyclonal (A0312), was purchased from ABclonal company, United States.

Animals and Study design

This study was conducted on 60 healthy adult male albino rats weighing 150-180gm, purchased from the

animal house of Faculty of Veterinary Medicine, Suez Canal University. They were acclimatized for 7 days before the expirement with free access to food and water, housed in clean cages at ordinary room temperature. After acceptance form the research and ethics committee of Faculty of Medicine, Suez Canal University, animals were randomized into six groups, ten animals each.

Group I (Control group) a) received a single intraperitoneal (I.P) injection of sterile water. Group II (Ginger extract group) received a single intragastric dose of Ginger extract (200 mg/kg) by gastric gavage[23]. Group III (Chitosan coated Ginger Nanoparticles group) received a single intragastric dose of CGNPs (50mg/kg)[13]. Group IV (Vancomycin group) received a single I.P injection of vancomycin (200mg/kg)[10]. Group V (Vancomycin + Ginger extract group) received a single I.P injection of Vancomycin followed directly by single dose of Ginger extract, both in the same previous doses as in groups II & IV[10,23]. Group VI (Vancomycin + CGNPs treated group) received a single I.P injection of Vancomycin followed directly by single dose of CGNPs, both in the same previous doses as in groups III & IV[10,13].

Specimens collection and histological techniques

At the end of the experiment, after 7 days, all animals were anesthetized with ether then sacrificed by cervical decapitation. Kidneys were extracted, fixed in 10% formaldehyde and embedded in paraffin, cut serially into 4µm thick sections for histological and immunohistochemical techniques[18].

I) Histological stains

- Haematoxylin and Eosin (H&E) stain: used for identification of the general architecture and histopathological changes in the renal cortex[24].
- Periodic Acid-Schiff (PAS) stain: used for demonstration of the polysaccharides in the basement membrane of glomerular capillary loops and proximal convoluted tubules and so, the apical brush border of their lining cells[24].

2) Immunohistochemical techniques

Tissues were deparafinized using xylene and rehydrated by multiple alcohol concentrations. After that, sections were washed by PBS and put in humidity chamber. Hydrogen peroxide was used to block endogenous peroxidase activity. Sections were washed by distilled water followed by PBS and left again in humidity chamber. Then, primary antibodies were added to be incubated at room temperature (30-60 min.):

- Anti-Caspase 3 antibody: to assess the apoptosis in the proximal renal tubular cells[10], appeared as brown cytoplasmic reaction.
- Anti-iNOS (inducible Nitric Oxide Synthase) antibody: to assess the inflammatory process in the renal tissue[25], appeared as brown cytoplasmic reaction.

For negative control, the same protocol was followed with omission of the primary antibody step.

For positive control, tonsils tissue was stained following the same protocol.

Histopathological and Morphometric study

1-Qualitative assessment

In the interstitial tissue and proximal convoluted tubules, the following histopathological changes were assessed[10]:

- Necrosis of the cells in the form of:
  - Cytoplasmic vacuolization.
  - Decreased acidophlilia.
  - Swelling, karyolysis and pyknosis of their nuclei.
- Tubular casts formation, tubular dilatation or even obstruction.
- Congested dilated blood capillaries and inflammatory cells infiltration in the interstitial tissue.

2-Quantitative assessment

The mean histological score was used to evaluate the previous histopathological changes in renal cortex according to the extent into the cortex, a grading scale of 0 to 4 was used (Table 1)[26]:

Table 1: The grading of the histopathological changes detected in the renal cortex

Grades	Extenstion in the cortex
0	No changes detected
1	≤25% cortex affected
2	>25% and ≤50% cortex affected
3	>50% and ≤75% cortex affected
4	>75% cortex affected

- The mean optical density of PAS-positive material (magenta color) in the basement membranes and brush borders.
- The mean optical density of Anti-Caspase 3 immunoreactivity in the proximal tubular epithelium (brownish cytoplasm).
- The mean optical density of Anti-iNOS immunoreactivity in the proximal tubular epithelium (brownish cytoplasm).

Statistical analysis

All data were coded and analysed using Statistical Package for the Social Sciences (SPSS) software version 22. Results were expressed in means and standard deviations using the One way ANOVA. Post hoc Tukey USD test was used to compare means, $P<0.05$ was considered statistically significant. The obtained data were presented in figures and tables.

RESULTS

Clinical sign

Animals appeared comfortable as evidenced by normal behavior and appetite. They were active with no clinical abnormalities during the period of the experiment.

Microscopic evaluation

Histological Results

a) Hematoxylin and eosin stain (H&E) results

Renal cortex sections from control group (I) showed normal architecture in the form of normal renal corpuscles, proximal convoluted tubules (PCT) and distal convoluted tubules (DCT) (Figures 2,3).

Sections of the renal cortex from group II and III showed normal architecture similar to that of the the control group (Figures 7,11). There was no significant statistical difference in the mean histological score of both groups, compared to control (Table 2).

Sections of renal cortex from Vancomycin group (IV) showed loss of cortex archeticture with severe necrotic changes to the PCT lining cells, luminal dilatation, casts formation and interstitial inflammation (dilated congested capillaries and inflammatory cells infiltration). However the renal corpuscles and DCT had no observed histopathological changes (Figures 15,16). About 80 % of animals in this group showed grade 4 of the histopathological changes and about 20% only showed grade 3. There was a significant increase in the mean histological score (2.80 ±0.422) of this group compared to the control group (Table 1).

Sections of renal cortex from group V showed evidence of improvements as compared to group IV (Figures 20,21). The PCT revealed normal cubical cells, but there were some tubules were lined with flat cells that showed vacuolated cytoplasm. There was also some luminal dialtation and casts formation. The histopathological changes were mild in 40 % of animals, moderate in 50 % and severe in 10% only. The mean histological score (1.70± 0.675) was significantly decreased compared to group IV and was significantly increased compared to control group (Table 2). Sections of renal cortex from group VI were nearly similar to that of control group. The mean histological score was significantly decreased compared to both group IVand V, but was non-significant compared to control group (Table 2). The PCT lumen had neither dilatation nor epithelial casts (Figures 25,26).

b) Periodic acid-Schiff reaction (PAS), Histogram 1

PAS-stained sections from control group revealed PAS positive material in the basement membranes of glomerular capillaries, Bowman's capsule, DCT and PCT, which were continuous and regular. and also in the brush border of PCT (Figure 4). The mean optical density of PAS magenta color of this group was 0.103 ± 0.019.

Groups II and III showed PAS positive material similar to that of control group (Figures 8,12). There was no significant statistical difference in the mean optical density of PAS positive material of these two groups (0.090 ± 0.009, 0.091 ± 0.041 respectivly), compared to control group. Group IV revealed PAS negative reaction in the brush border of the proximal convoluted tubules and their basement membranes were highly disrupted and irregular, also there was magenta positive PAS casts in the PCT (Figure 17). However the basement membranes of the renal corpuscles and DCT appeared normal. There was a statistically significant decrease in the mean optical density of the positive PAS magenta color of this group, compared to control group.

Sections of renal cortex from group V showed positive magenta color reaction in the basement membranes of renal corpuscles, PCT and DCT but it decreased in PCT brush border (Figure 22). There was a statistically significant increase in the mean optical density of PAS positive material in this group (0.072± 0.013) compared to group IV but it was significantly decreased compared to control group. Group VI PAS-stained sections revealed a PAS positive reaction in the brush border of PCT and the basement membranes similar to that of control group (Figure 27). There was statistically significant increase in the mean optical density of PAS magneta colour (0.082 ± 0.009) compared to group IV but there was no statistical significant difference compared to group V and control group.

Immunohistochemical Results

a) Anti-Caspase 3 immunostaining, Histogram 2

The stained sections from groups I, II and III renal cortex showed only a little positive brown reaction in the cytoplasm of few renal tubules (Figures 5,9,13). There was no statistical difference in between these groups.

Group IV showed a marked positive cytoplasmic reaction in the PCT (Figure 18), with significant increase in the mean optical density of the immunoreaction (0.078 ± 0.005) compared to control.

Group V showed a moderate positive cytoplasmic reaction in the PCT (Figure 23) which was not significant compared to group IV but there was statistically significant increase compared to control group. The mean optical density of the immunoreaction was 0.075± 0.008. While the renal cortex from group VI showed little positive brown cytoplasmic reaction, similar to that of control group (Figure 28). This immunoreactivity was significantly decreased compared to groups IV and V.

b) Anti-iNOS immunostaining, Histogram 3

The control group renal cortex showed a mild positive brown reaction in the cytoplasm of few DCT and PCT (Figure 6), and so group II and III (Figures 10,14 respectivly). There was no significant statistical difference between these groups.

Group IV showed a strong positive brown cytoplasmic reaction in the PCT cells (Figure 19) with a significant increase in the mean optical density of the iNOS immunoreaction (0.0815 ± 0.014) compared to the control group.

Group V revealed moderate positive cytoplasmic reaction in some cortex tubules (Figure 24), with the mean optical density was 0.060 ± 0.008. The immunoreactivity of this group was significantly decreased compared to group V but was significantly increased compared to the control group.

Group VI showed mild positive cytoplasmic reaction in some tubules (Figure 29). The mean optical density of the immunoreaction (0.040 ± 0.008) was significantly less than groups IV and V. There was no statistical significant difference between the iNOS immunoreaction in this group and the control group.

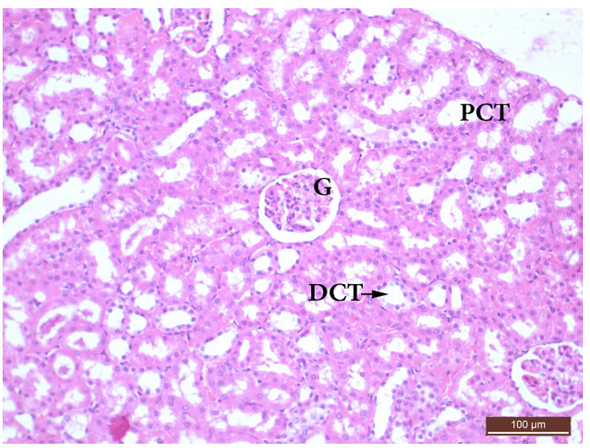

Fig. 2: A photomicrograph of renal cortex from group I showing normal cortex archeticture, renal corpuscle (G), proximal convoluted tubules (PCT) and distal convoluted tubules (DCT). (H&E x 200)

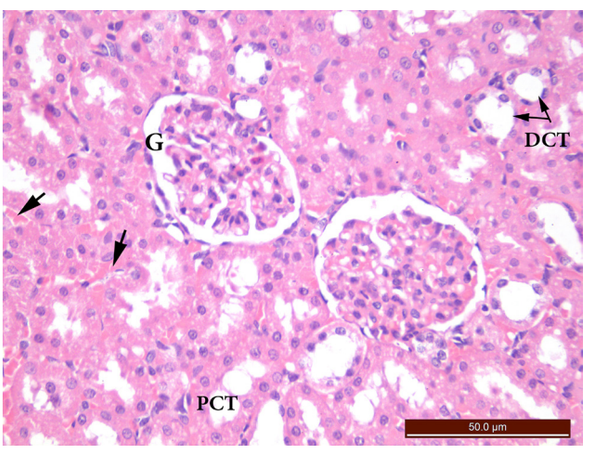

Fig. 3: A photomicrograph of renal cortex from group I showing normal renal corpuscle has a glomerulus(G) surrounded with Bowman's space and lined with simple squamous cells. PCT is lined with high cubical cells that have rounded vesicular nuclei and deep acidophilic cytoplasm. DCT is lined with low cubical cells that have rounded more dense nuclei than PCT and less acidophilic cytoplasm. Normal blood capillaries (arrows). (H&E x 400)

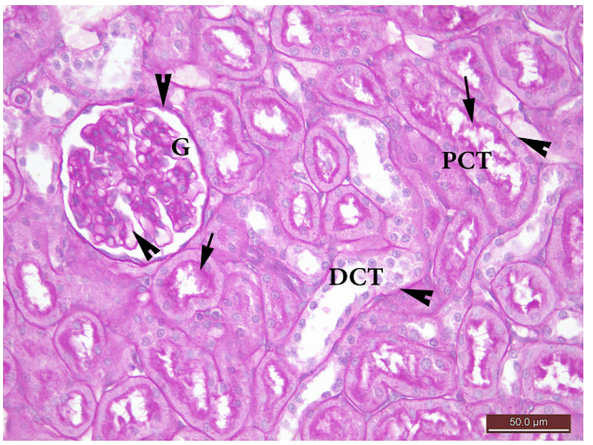

Fig. 4: A photomicrograph of the renal cortex from group I showing PAS positive material in the basement membranes of DCT, PCT, glomerular apillaries (G) and Bowman's capsule of the glomeruli (arrow heads).. These membranes are regular and continuous. Positive reaction in the brush border of PCT is shown (arrow). (PAS x 400)

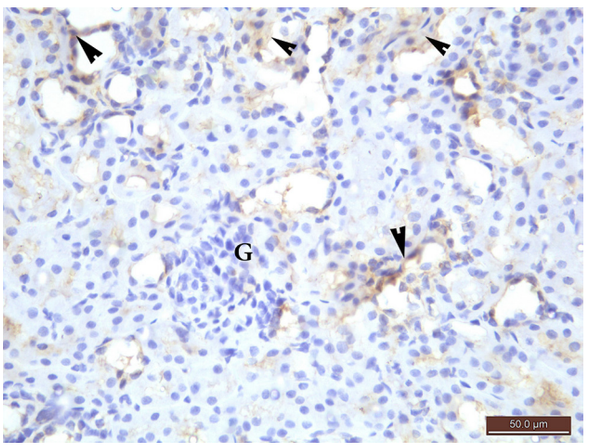

Fig. 5: A photomicrograph of renal cortex from group I showing mild immunoreactivity of anti-caspase3 in the form of brownish positive reaction in the cytoplasm of few renal tubules (arrow heads). (Anti-Caspase3 immunostainning x 400)

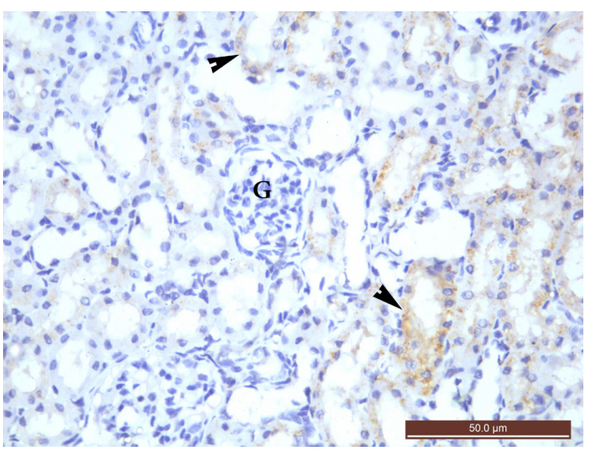

Fig. 6: A photomicrograph of renal cortex from group I showing mild immunoreactivity of anti-iNOS in the form of brownish positive reaction in the cytoplasm of few renal tubules (arrow heads). (Anti-iNOS immunostainning x 400)

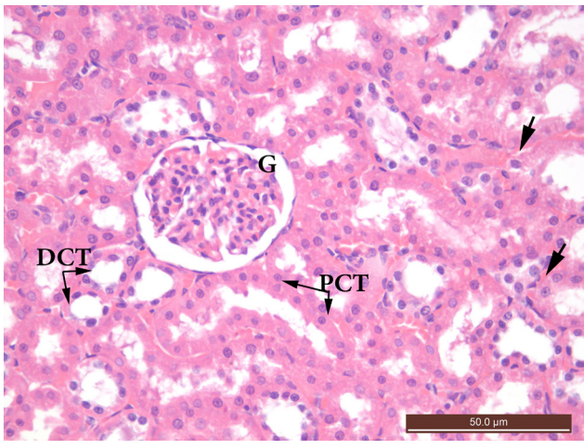

Fig. 7: A photomicrograph of renal cortex from group II showing normal cortex archeticture, renal corpuscle (G), proximal convoluted tubules (PCT) and distal convoluted tubules (DCT). (H&E x 400)

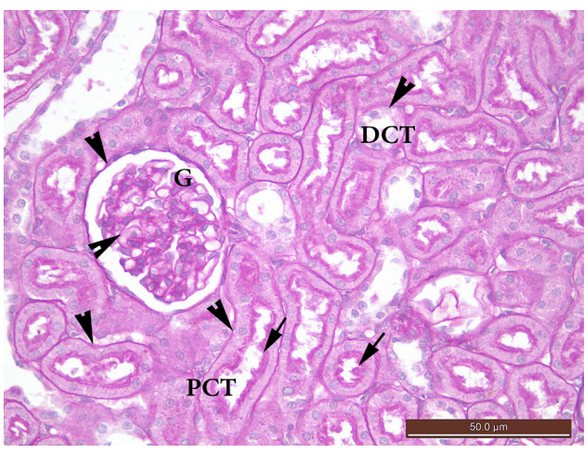

Fig. 8: A photomicrograph of the renal cortex from group II showing PAS positive material in the basement membranes of the glomerular capillaries (G) Bowman's capsule, PCT, DCT (arrow heads) and also in the brush border of PCT (arrow). (PAS x 400)

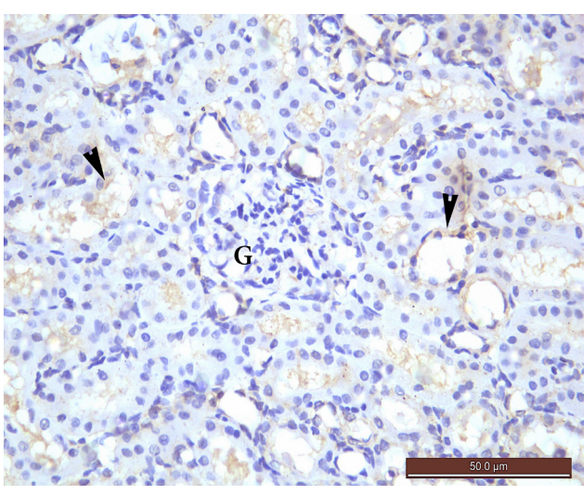

Fig. 9: A photomicrograph of renal cortex from group II showing mild immunoreactivity of Anti-Caspase3 in the form of brown positive reaction in the cytoplasm of few renal tubules similar to group I (black arrows). (Anti-Caspase3 immunostainning x 400)

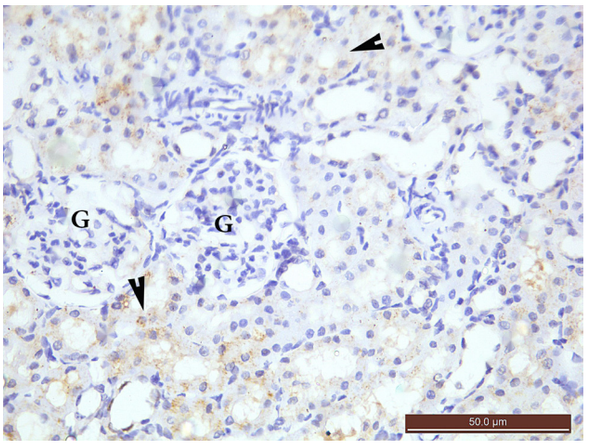

Fig. 10: A photomicrograph of renal cortex from group II showing mild immunoreactivity of Anti-iNOS in the form of brown positive reaction in the cytoplasm of few renal tubules similar to group I (arrow head). (Anti-iNOS immunostainning x 400)

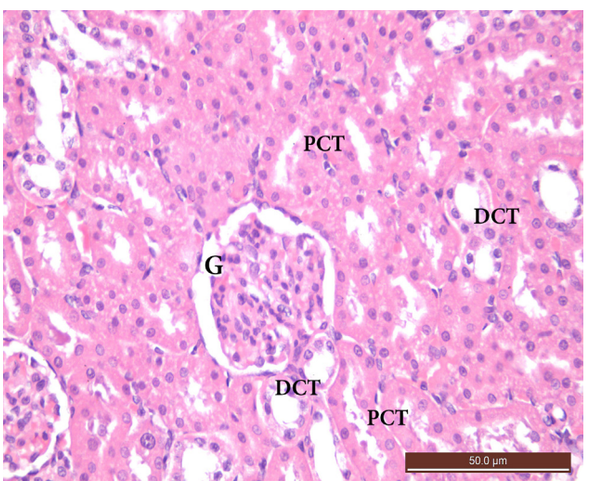

Fig. 11: A photomicrograph of renal cortex from group III showing normal cortex archeticture, renal corpuscle (G), proximal convoluted tubules (PCT) and distal convoluted tubules (DCT). (H&E x 400)

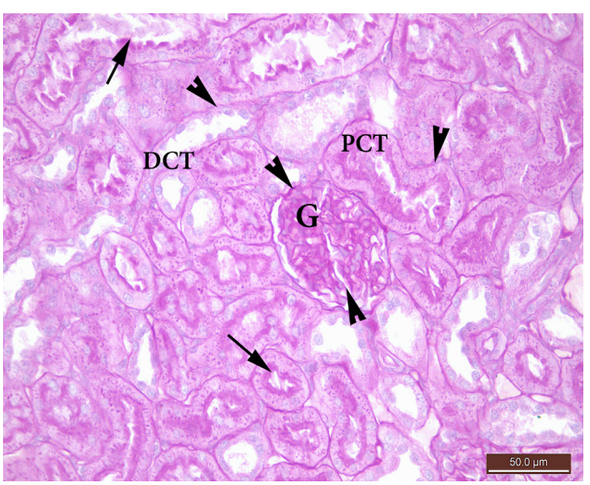

Fig. 12: A photomicrograph of the renal cortex from group III showing PAS positive material similar to group I. (PAS x 400)

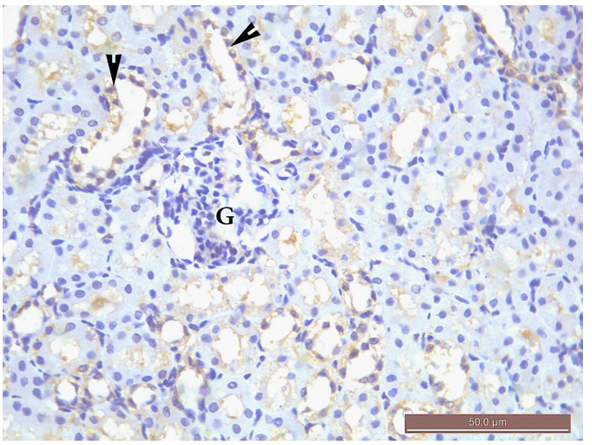

Fig. 13: A photomicrograph of renal cortex from group III showing mild immunoreactivity of Anti-Caspase3 in the cytoplasm of few renal tubules similar to group I (anti-caspase3 immunostainning x 400)

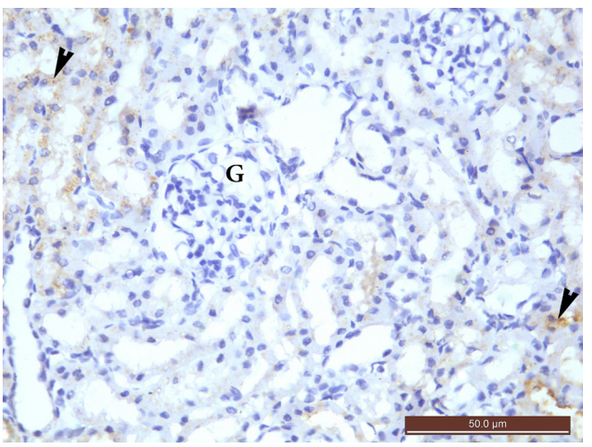

Fig. 14: A photomicrograph of renal cortex group III showing mild immunoreactivity of Anti-iNOS in the cytoplasm of few tubules similar to group I (arrow heads). (Anti-iNOS immunostainning x 400)

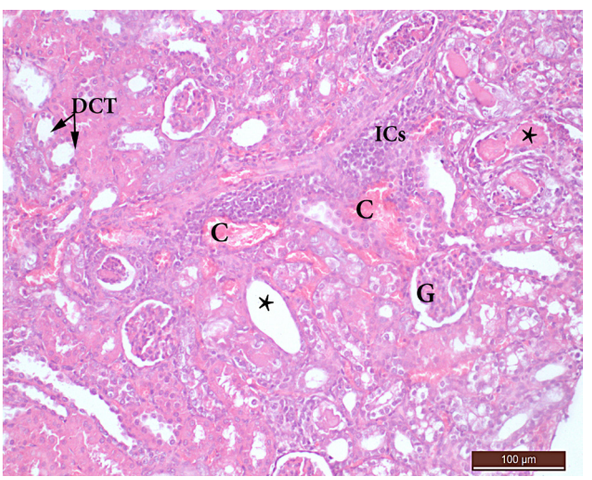

Fig. 15: A photomicrograph of renal cortex from group IV showing loss of archeticture, congested dilated capillaries (C), inflammatory cellular infiltration (ICs). PCT show dilated lumen or obliteration with casts formation (*). Normal renal corpuscles (G) and DCT. (H&E x 200)

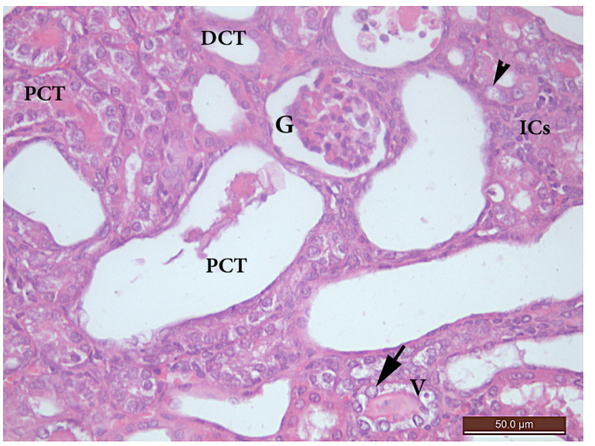

Fig. 16: A photomicrograph of renal cortex from group IV showing necrotic changes in PCT in the form of decrease in cytoplasmic eosinophilia with epithelial vacuolization (V), casts formation inside the lumen of some tubules, dilatation of others with flattening of their lining cells and pyknotic nuclei. Some cells show nuclear swelling with chromatin margination (arrow), others show karyolysis and loss of nuclei (arrow head). The renal interstitium shows inflammatory infiltration (ICs) and cellular depris. (H&E x 400)

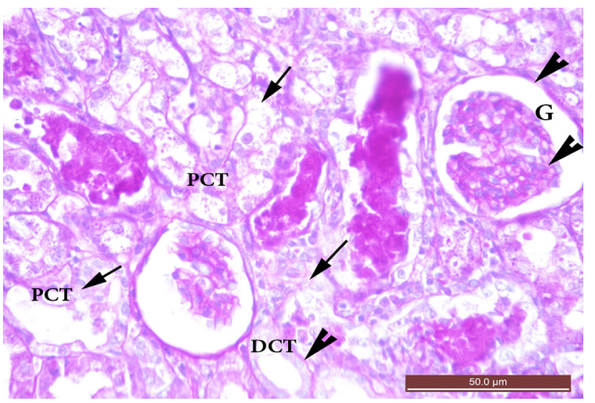

Fig. 17: A photomicrograph of the renal cortex from group IV showing decrease in the magenta reaction of basement membrane of PCT with absence of their brush borders (arrows). A positive reaction in the epithelial casts is also shown. normal PAS positive reaction in the basement membranes of glomerular capillaries (G) and the surrounding Bowman's capsule, and of DCT (arrow heads). (PAS x 400)

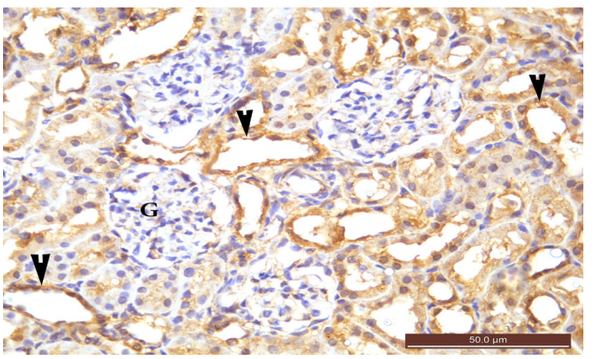

Fig. 18: A photomicrograph of renal cortex from group IV showing increase in the immunoreactivity of Anti-Caspase3 in the form of strong brown positive reaction in the cytoplasm of the lining cells of PCT which appear with dilated luminae, compared to group I (arrow heads). (Anti-Caspase3 immunostainning x 400)

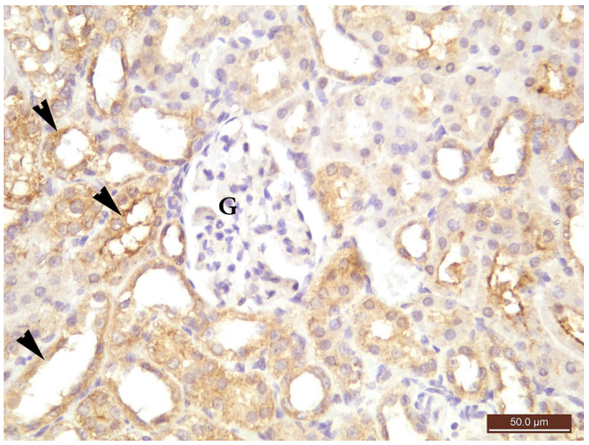

Fig. 19: A photomicrograph of renal cortex from group IV showing increase in the immunoreactivity of Anti-iNOS, compared to group I, in the form of strong brown positive reaction in the cytoplasm of the cells lining PCT (arrow heads) which appear with dilated luminae. (Anti-iNOS immunostainning x 400)

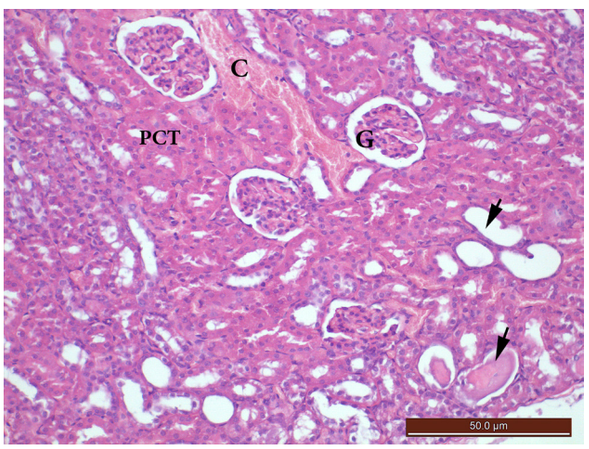

Fig. 20: A photomicrograph of renal cortex from group V showing some improvement compared to group IV with normal PCT. Still there are some PCT show wide lumen either with casts or empty (arrows). Dilated congested capillary is also shown (C). (H&E x 200)

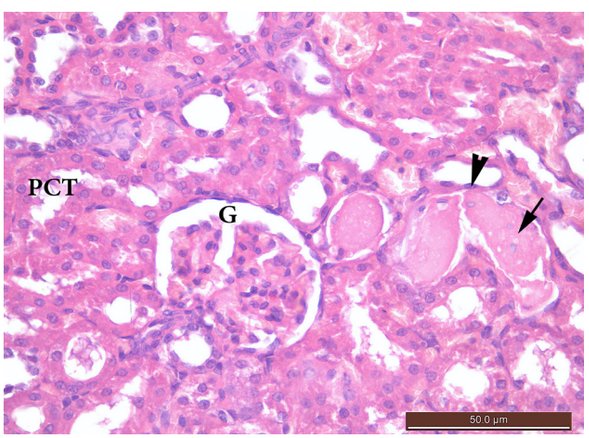

Fig. 21: A photomicrograph of renal cortex from group V showing normal PCT with its high cubical cells, deep acidophilic cytoplasm and rounded vesicular nuclei. Also, some PCT is lined with flat cells which have pyknotic nuclie (arrow head), others have luminal casts (arrow). (H&E x 400)

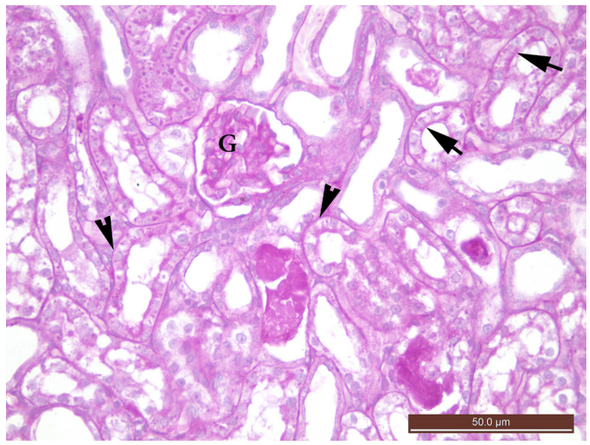

Fig. 22: A photomicrograph of the renal cortex from group V showing decrease in PAS positive material, compared to group I, in the basement membranes (arrows) and the brush borders of PCT (arrows). Also, some tubules still show a PAS positive casts. (PAS x 400)

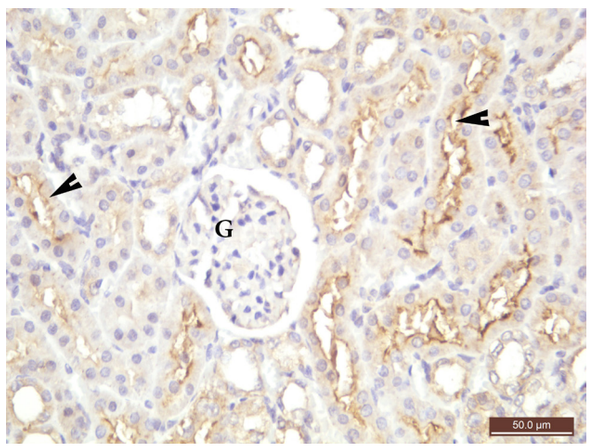

Fig. 23: A photomicrograph of renal cortex from group V showing decrease in the immunoreactivity of Anti-Caspase3, in the cytoplasm of PCT lining cells (arrow heads) compared to group IV, but the reaction is still more than that of the control group. (Anti-Caspase3 immunostainning x 400)

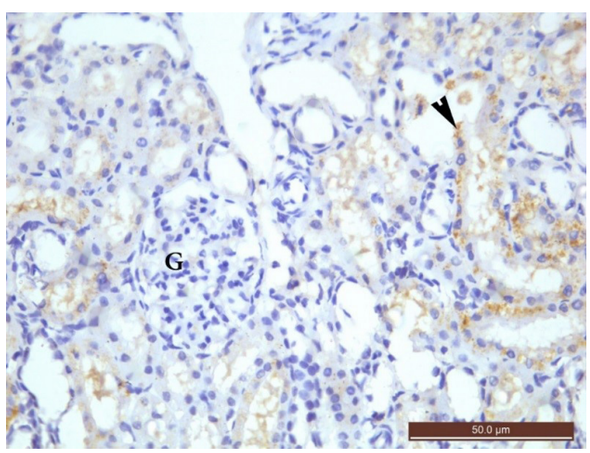

Fig. 24: A photomicrograph of renal cortex from group V showing decrease in the immunoreactivity of Anti-iNOS in the cytoplasm of PCT lining cells, compared to group IV , but the reaction is still more than that of the control group. (Anti-iNOS immunostainning x 400)

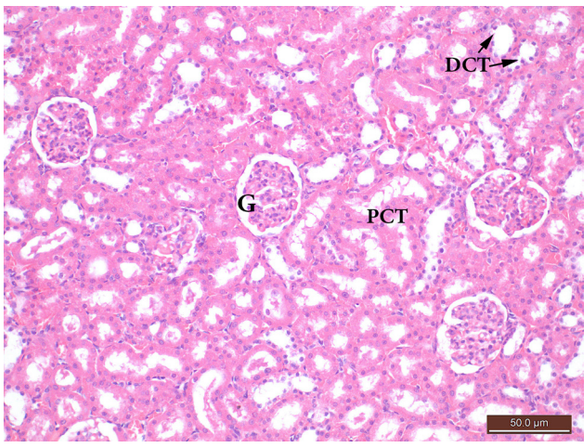

Fig. 25: A photomicrograph of renal cortex from group VI showing normal renal cortex archeticture, similar to group I. (H&E x 200)

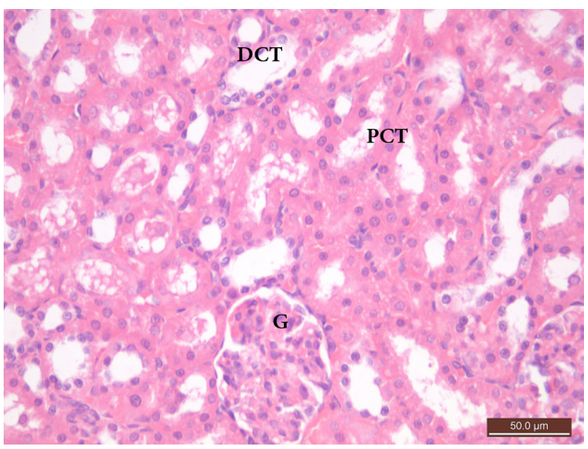

Fig. 26: A photomicrograph of renal cortex from group VI showing improvement with normal PCT have high cubical cells with deep acidophilic cytoplasm and vesicular rounded nuclei. (H&E x 400)

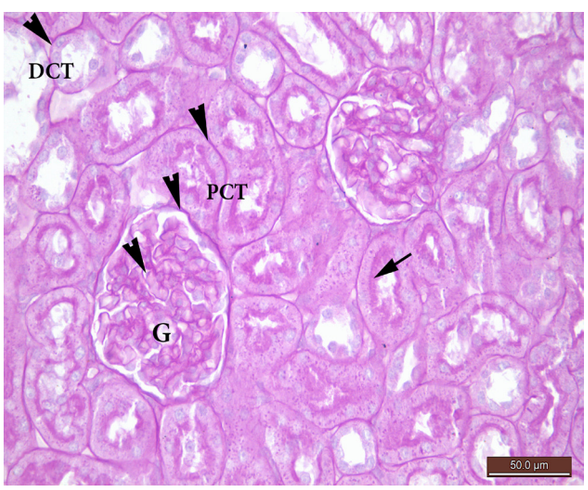

Fig. 27: A photomicrograph of the renal cortex from group VI showing normal PAS positive material, similar to group I, in the basement membranes of the glomerular capillaries (G) Bowman's capsule, PCT, DCT (arrow heads) and also in the brush border of PCT (arrow). (PAS x 400)

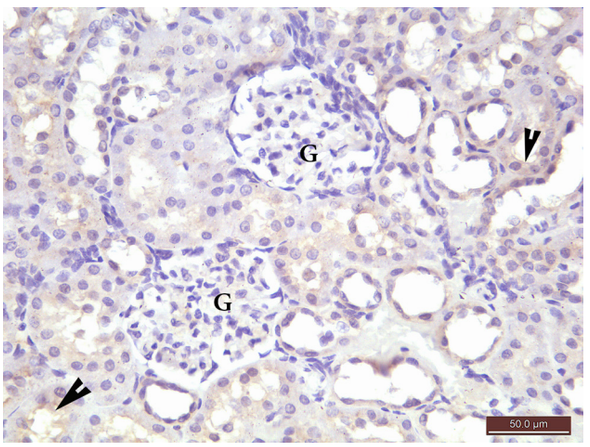

Fig. 28: A photomicrograph of renal cortex from group VI showing marked decrease in the immunoreactivity, compared to group IV. Mild brownish positive reaction in the cytoplasm of the cells lining few renal tubulrs (arrow head), nearly similar to control group. (Anti-Caspase3 immunostainning x 400)

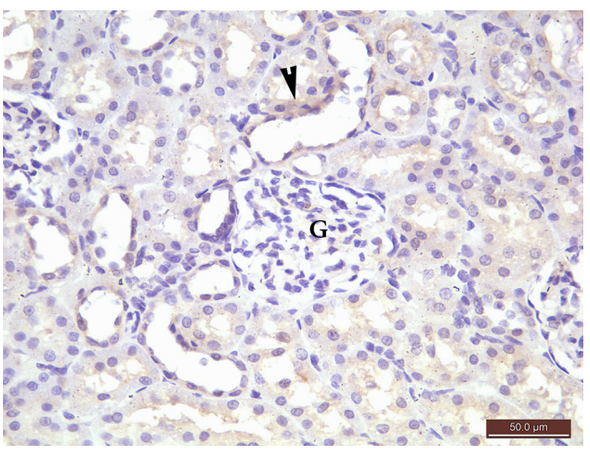

Fig. 29: A photomicrograph of renal cortex from group VI showing marked decrease in the immunoreactivity, compared to group VI, in the cytoplasm of cells lining few tubules (arrow head), nearly similar to control group. (Anti-iNOS immunostainning x 400)

Table 2: The mean and standard deviation of the histological score of the H&E-stained renal cortex in different experimental groups

upsGroups	Mean ±SD
I	0
II	0
III	0
IV	2.8±0.42*
V	1.70± 0.675lq
VI	0 km

ANOVA and Post-Hoc Tukey HSD tests. Statistically significant at $p < 0.05$.
*Significant difference between group IV and I
l Significant difference between group V and I
q Significant difference between group V and IV
k Significant difference between group VI and IV
m Significant difference between group VI and V

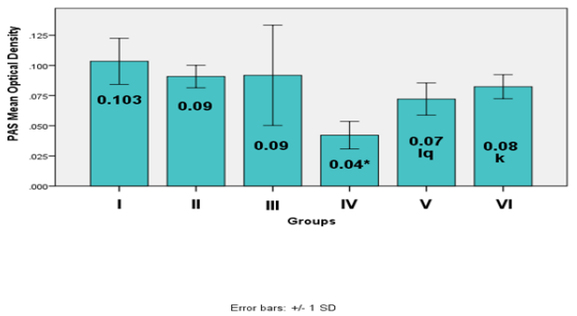

Histogram 1: The mean and standard deviation of the optical density of magenta color of PAS-renal cortex in different experimental groups

ANOVA and Post-Hoc Tukey HSD tests. Statistically significant at $p < 0.05$. *Significant difference between group IV and I - l Significant difference between group V and I - q Significant difference between group V and IV - k Significant difference between group VI and IV

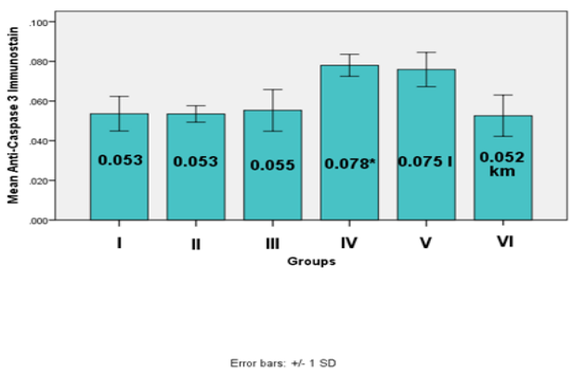

Histogram 2: The mean and standard deviation of the optical density of the Anti-Caspase3 immunoreactivity in different experimental groups

ANOVA and Post-Hoc Tukey HSD tests. Statistically significant at $p < 0.05$. *Significant difference between group IV and I - l Significant difference between group V and I - q Significant difference between group V and IV - k Significant difference between group VI and IV

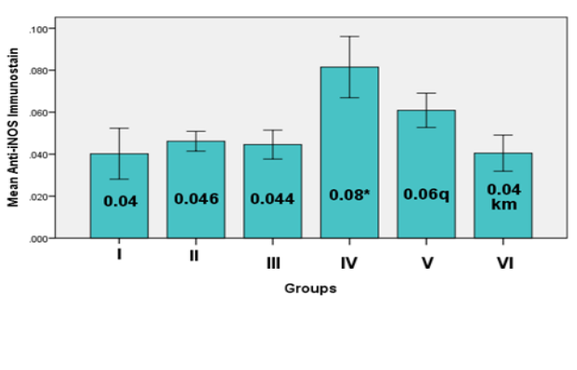

Histogram 3: The mean and standard deviation of the optical density of the Anti-iNOS immunoreactivity in different experimental groups

ANOVA and Post-Hoc Tukey HSD tests. Statistically significant at $p < 0.05$. *Significant difference between group IV and I - l Significant difference between group V and I - q Significant difference between group V and IV - k Significant difference between group VI and IV

DISCUSSION

Vancomycin is a widely used antibiotic, it is the first line in the treatment of multiple bacterial infections, caused by aerobic and anaerobic gram-positive bacteria. It is mostly used in staphylococcal infections which are resistant to other types of antibiotics[27]. Nephrotoxicity is considered to be one of the major adverse effects of vancomycin treatment especially after its intravenous administration[28]. Little attention has been paid to the use of natural substances, such as ginger which is known for its potent antioxidant and anti-inflammatory properties, to protect against such a nephrotoxicity.

The present study was designed to investigate and compare the possible protective effect of Chitosan coated Ginger Nanoparticles (CGNPs) and Ginger against VCM-induced nephrotoxicity in adult male albino rats, using histological and immunohistochemical techniques.

The current work revealed severe histopathological changes in Vancomycin treated group (Group IV). H&E stained renal cortex sections from this group showed; significant loss of architecture, after 7 days of vancomycin injection. The histopathological changes were including only proximal convoluted tubules in addition to congested dilated capillaries and interstitial inflammatory cell infiltration. The PCT showed necrosis, luminal dilatation and appearance of hyaline casts. These findings were consistent with those of Pais *et al*., 2019 who used the same dose of VCM as us and reported that histopathological changes were mainly to epithelial cells of proximal convoluted tubules such as vacuolization, desquamation, atrophy and tubular necrosis with inflammatory cellular infiltration[29]. Similar results were described by Takigawa *et al*., 2019 who used vancomycin by doubling the dose. They noticed significant renal tubular necrosis with epithelial desquamation and formation of hyaline casts[18].

The PAS stained sections revealed decrease in the PAS positive material in the brush border and basement membrane of the PCT with significant decrease in the mean optical density compared to control group. Similar findings were reported by Takigawa *et al*., 2017 who attributed this decrease due to atrophy in the basement membrane and the brush border. They also found hyaline casts, which were also positively stained as in our study, caused by severe tubular epithelial desquamation[18]. Stokes, 2017 added that hyaline casts were formed due to some precipitates from vancomycin and uromodulin (Tamm Horsfall glycoprotein, which is normaly secreted by PCT cells into urine)[30].

The Anti-Caspase 3 immunostained sections of this group showed a significant increase in the positive reaction of the cytoplasm of the cells lining PCT, compared to control group (the mild reaction appeared in control group in few tubules is due to normal physiological turnover). It was reported that vancomycin induced apoptosis through elevation of free radicals level inside the cells resulting in oxidation of the mitochondrial membrane with a subsequent release of Cytochrome C into the cytosol activating caspase cascade[2].

The Anti-iNOS immunostained sections revealed also significant increased reaction in the cytoplasm of PCT cells, compared to control group. This result was similar to other researchers who confirmed the elevation of iNOS levels in rats that were treated by vancomycin for the same dose and duration[31]. These findings were also demonsterated by other researchers, who found that the oxidative stress caused by vancomycin directly increased the iNOS enzyme[32].

Studies revealed involvement of oxidative phosphorylation in Vancomycin pathophysiology with release of oxygen free radicals and inhibition of the action of defensive antioxidant enzymes such as superoxide dismutase and catalase. This inhibition increases the levels of mitochondrial peroxide which followed by change of the membrane potentiality with activation of the apoptotic caspase pathway[4,5]. The oxidative stress also causes proteins, lipids and DNA oxidation ending in eliciting direct inflammation, congetion, cellular infiltration and cell damage[32].

It was reported that Vancomycin affects mainly the PCT, as it is excreted by glomerular filtration and active tubular secretion which causes drug accumulation in the epithelial cells of these tubules. Additionally, Vancomycin inhibits the function of P-glycoprotein which acts as efflux transporter that controls Vancomycin reabsorption and secretion resulting in more drug accumulation and further nephrotoxicity[33].

Vancomycin with Ginger group (V), the H&E results of this group were nearly similar to control group. Most sections showed preserved architecture of the renal cortex with significant improvement in the histopathological changes compared to group IV. There was significant decrease in the mean histological score compared to group IV, but, was significantly increased compared to control group. Some PCT still showed tubular necrosis and epithelial shedding with subsequent casts formation and luminal dilatation. Similar results were described by Kandemir *et al*., 2018 who confirmed the role of zingerone (the active ingredient of ginger) in improving the histopathological changes in PCT. They noticed that daily oral dose of Zingerone could decrease the epithelial desquamation, luminal dilatation and casts formation[10].

Additionally, many studies were conducted to demonstrate the role of ginger in alleviating drug induced nephrotoxicity. A study investigated the role of oral Ginger extract against Gentamycin induced nephrotoxicity concluded that Ginger could decrease the histopathological changes in the glomeruli and PCT[23]. Moreover Ali *et al*., 2015 used Ginger against Cisplatin induced renal injury in rats and found reduction in tubular necrosis and epithelial shedding with no luminal dilatation[34].

The PAS stained sections revealed positive magenta color in the basement membrane and the brush border of proximal convoluted tubules, nearly similar to control group. Our results were consistent with the results of a study observed the normal magenta color in rats renal sections with glycerol induced nephrotoxicity after treatment with Ginger[35].

The Anti-Caspase 3 immunostained sections showed a significant decrease in the immunoreactivity in the cytoplasm of the cells lining PCT, compared to group IV, but still more than that of control group. Our results were in accordance with Baiomy and Mansour, 2016 who demonstrated decreased immunoreactivity for Caspase 3 in rabbits treated by ginger against cadmium-induced nephrotoxicity[36]. It was reported that Ginger prevents Caspase 3 activation and apoptosis through decreasing free radical levels, and so Cytochrome C release from the mitochondria[37].

The Anti-iNOS immunostained sections showed significant decrease in the immnoreactivity in the cytoplasm of the PCT compared to group IV. Our results were in agreement with Kucukler *et al*., 2020 who investigated the level of iNOS in rats treated by zingerone against vancomycin-induced hepatotoxicity. They noticed low level of serum iNOS[38].

Ginger was reported to have potent anti-inflammatory effect similar to NSAIDs in lowering the nitric oxide (NO) levels and treating joint edema[39,40]. Moreover, ginger was found to reduce the pro-inflammatory mediators such as COX-2 and iNOS, which is responsible for the production of NO[41]. The protective effect of Ginger against drug induced nephrotoxicity might be attributed to its ability to ameliorate apoptosis and necrosis in PCT through lowering the oxidative stress. Ginger increases the antioxidant enzymes such as superoxide dismutase, catalase, glutathione level and glutathione peroxidase and decreases the oxidative stress marker malondialdehyde. It also lowers the reactive oxygen species by donating electrons to free radicals leaving them stable[42]. Additionay Ginger lowers renal tubular inflammation through inhibiting the production of pro-inflammatory cytokines, such as tumor necrosis factor-alpha and interleukin-1β, and decreases the leukotriene biosynthesis by inhibiting the arachidonate 5-lipoxygenase enzyme[43,44].

Vancomycin with ginger nanoparticles treated group (VI) showed an improvement of all the histological and immunohistochemical findings compared to both group IV and group V. The H&E sections, results revealed significant decrease in the mean histological score compared to groups IV and V. The renal structure was similar to control group without tubular dilatation or casts formation. Our results were in agreement with Bakr, 2019 who compared between the protective role of GNPs and Ginger extract against acetaminophen induced hepato-renal toxicity. He found that GNPs had better results than ginger extract in improving the tubular epithelial vacuolization, luminal cast formation, vascular congestion and inflammatory cellular infiltration[45]. Abd-Elrhman *et al*., 2020 also confirmed the previous results through investigating the effect of GNPs against carbon tetrachloride induced hepatorenal toxicity

in rats, they found improvement in epithelial vacuolization and interstitial inflammatory infiltration[46].

PAS stained sections showed a positive PAS material in the basement membrane and the brush border of PCT which was nearly similar to control group. GNPs were reported to have a powerful effect in epithelial healing when given orally for 7 days by Zhang *et al*., 2018 who suugested that 6-Shagols could suppress the inflammatory mediators and enhance cellular repair[47].

The Anti-Caspase 3 immunostained results from this group revealed significant decrease in immunoreactivity compared to groups IV and V and similar to that of control group, indicating decreased apoptotic activity in epithelial cells of proximal convoluted tubules. It was reported that GNPs modulate the apoptotic activity in rats with dioxin induced cancer, increased the expression of anti-apoptotic genes and decreased the expression of pro-apoptotic ones such as Bcl-2 and Bax, respectively[13].

The Anti-iNOS immunostained sections showed positive reaction in the cytoplasm of cells of proximal convoluted tubules, nearly similar to control group, with significant decrease compared to groups IV and V. This was in accordance with Zhang *et al*., 2018 who reported that GNPs could relieve the symptoms of colitis and enhance healing of the ulcerated mucosa by lowering the expression levels of pro-inflammatory iNOS mediator[47].

This better effect of CGNPs compared to Ginger extract in our study, could be attributed to their high bioavailability. Therefore, small amounts of these water soluble nanoparticles could be absorbed after oral administration, unlike ginger extract which needs frequent administration to produce a significant effect[15]. Additionally, Zhuang *et al*., 2015 noticed that GNPs have higher antioxidant properties, than Ginger extract, against free radicals. This could be belonged to the role of shogaols, ginger active compounds, which are found in GNPs in a bind form not in a free one as in ginger. Accordingly, shogaols in GNPs can produce a better effect than those found in Ginger extract[48].

So in the present study, we can conclude that administration of Chitosan coated Ginger Nanoparticles, daily for 7 days, promoted more improvement than Ginger extract in morphology of Renal cortex against Vancomycin induced nephrotoxicit toxicity in adult male albino rats.

CONFLICT OF INTERESTS

There are no conflicts of interest.

REFERENCES

1. Zeng D, Debabov D, Hartsell TL, Cano RJ, Adams S, Schuyler JA, McMillan R and Pace JL. Approved glycopeptide antibacterial drugs: mechanism of action and resistance. Cold Spring Harbor perspectives in medicine. (2016) 6(12).
2. Sakamoto Y, Yano T, Hanada Y, Takeshita A, Inagaki F, Masuda S, Matsunaga N, Koyanagi S, and Ohdo S. Vancomycin induces reactive oxygen species-dependent apoptosis via mitochondrial cardiolipin peroxidation in renal tubular epithelial cells. Euro J pharmacol. (2017) 800:48-56.
3. Boswihi SS and Udo EE. Methicillin-resistant Staphylococcus aureus: an update on the epidemiology, treatment options and infection control. Current Medicine Research and Practice. (2018) 8(1):18-24.
4. Bamgbola O. Review of vancomycin-induced renal toxicity: an update. Therapeutic advances in endocrinology and metabolism. (2016) 7(3):136-47.
5. Filippone EJ, Kraft WK and Farber JL. The nephrotoxicity of vancomycin. Clinical Pharmacology & Therapeutics. (2017) 102(3):459-69.
6. Vora S. Acute renal failure due to vancomycin toxicity in the setting of unmonitored vancomycin infusion. Baylor University Medical Center Proceedings. (2016) 29 (4): 412-413. Taylor & Francis.
7. Öktem F, Arslan MK, Ozguner F, Candir Ö, Yilmaz HR, Ciris M and Uz E. In *vivo* evidences suggesting the role of oxidative stress in pathogenesis of vancomycin-induced nephrotoxicity: protection by erdosteine. Toxicology. (2005) 215(3):227-33.
8. Ocak S, Gorur S, Hakverdi S, Celik S and Erdogan S. Protective effects of caffeic acid phenethyl ester, vitamin C, vitamin E and N-acetylcysteine on vancomycin-induced nephrotoxicity in rats. Basic & clinical pharmacology & toxicology. (2007) 100(5):328-33.
9. Saagar Akundi YR, Perry GK, Fike DS and Mnjoyan S. Nephrotoxicity in recipients of vancomycin vs. vancomycin with vitamin C. International Journal of Medicine and Pharmacology. (2015) 3(2):1-5.
10. Kandemir FM, Yildirim S, Kucukler S, Caglayan C and Mahamadu A, Dortbudak MB. Therapeutic efficacy of zingerone against vancomycin-induced oxidative stress, inflammation, apoptosis and aquaporin 1 permeability in rat kidney. Biomedicine & Pharmacotherapy. (2018) 105:981-91.
11. Kota N, Krishna P and Polasa K. Alterations in antioxidant status of rats following intake of ginger through diet. Food chemistry. (2008) 106(3):991-6.
12. Korni FM and Khalil F. Effect of ginger and its nanoparticles on growth performance, cognition capability, immunity and prevention of motile Aeromonas septicaemia in Cyprinus carpio fingerlings. Aquaculture Nutrition. (2017) 23(6):1492-9.
13. Abdu SB, Abdu F and Khalil WK. Ginger nanoparticles modulate the apoptotic activity in male rats exposed to dioxin-induced cancer initiation. International journal of pharmacology. (2017) 13(8):946-57.

14. Ansari SH, Islam F and Sameem M. Influence of nanotechnology on herbal drugs: A Review. Journal of advanced pharmaceutical technology & research. (2012) (3):142.

15. Thapa RK, Khan GM, Parajuli-Baral K and Thapa P. Herbal medicine incorporated nanoparticles: advancements in herbal treatment. Asian journal of biomedical and pharmaceutical sciences. (2013) 3(24).

16. Chamundeeswari M, Jeslin J and Verma ML. Nanocarriers for drug delivery applications. Environmental Chemistry Letters. (2019) 17(2):849-65.

17. Mohammed MA, Syeda J, Wasan KM and Wasan EK. An overview of chitosan nanoparticles and its application in non-parenteral drug delivery. Pharmaceutics. (2017) 9(4):53.

18. Takigawa M, Masutomi H, Shimazaki Y, Arai T, Lee J, Ishii T, Mori Y and Ishigami A. Age-dependent changes in vancomycin-induced nephrotoxicity in mice. Journal of toxicologic pathology. (2019) 32(1):57-66.

19. Prasad S and Tyagi AK. Ginger and its constituents: role in prevention and treatment of gastrointestinal cancer. Gastroenterology research and practice. (2015) 2015.

20. Arulvasu C, Mani KA, Chandhirasekar D and Prabhu D, Sivagnanam SH. Effect of dietary administration of Zingiber officinale on growth, survival and immune response of Indian major carp, Catla catla (Ham.). International Journal of Pharmacy and Pharmaceutical Sciences. (2013) 5(2):108-15.

21. Saber AS, Sobhy EE, Yosry AO and Ahmed ME. Impact of ginger aqueous extract on carbimazole induced testicular degenerative alterations and oxidative stress in albino rats. Journal of Costal Life Medicine. (2017) 5(4):167-73.

22. Pedroso-Santana S and Fleitas-Salazar N. Ionotropic gelation method in the synthesis of nanoparticles/ microparticles for biomedical purposes. Polymer International. (2020) 69(5):443-7.

23. Nasri H, Nematbakhsh M, Ghobadi S, Ansari R, Shahinfard N and Rafieian-Kopaei M. Preventive and curative effects of ginger extract against histopathologic changes of gentamicin-induced tubular toxicity in rats. International journal of preventive medicine. (2013) 4(3):316.

24. Suvarna, K.S., Layton, C., Bancroft, J.D. 2013, Theory and practice of histological techniques, 7th edition. Elsevier Churchill Livingston, Edinburgh.

25. Sadeeshkumar V, Arul D and Ravichandran S. Protective effects of gallic acid in the renal markers, histopathology and immunohistochemical studies on vancomycin induced nephrotoxic rats. International journal of Advanced Life Sciences. (2013) 6(3):356-64.

26. Mohebbati R, Shafei MN, Beheshti F, Soukhtanloo M and Roshan NM, Anaeigoudari A, Parhizgar S, Hosseinian S, Khazdeir MR, Rad AK. Mixed hydroalcoholic extracts of Nigella sativa and Curcuma longa improves adriamycin-induced renal injury in rat. Saudi journal of kidney diseases and transplantation. (2017) 28(6):1270.

27. Jeffres MN. The whole price of vancomycin: toxicities, troughs, and time. Drugs. (2017) 77(11):1143-54.

28. Zamoner W, Prado IR, Balbi AL and Ponce D. Vancomycin dosing, monitoring and toxicity: Critical review of the clinical practice. Clinical and Experimental Pharmacology & Physiology. (2019) 46(4):292-301.

29. Pais GM, Liu J, Avedissian SN, Xanthos T, Chalkias A, d'Aloja E, Locci E, Gilchrist A, Prozialeck WC, Rhodes NJ and Lodise TP. Urinary biomarker and histopathological evaluation of vancomycin and piperacillin-tazobactam nephrotoxicity in comparison with vancomycin in a rat model and a confirmatory cellular model. Journal of Antimicrobial chemotherapy. (2019) 1:568907.

30. Stokes, M. Barry. Vancomycin in the kidney—a novel cast nephropathy. Journal of the American Society of Nephrology. (2017): 1669-1670.

31. Qu S, Dai C, Lang F, Hu L, Tang Q, Wang H, Zhang Y and Hao Z. Rutin attenuates vancomycin-induced nephrotoxicity by ameliorating oxidative stress, apoptosis, and inflammation in rats. Antimicrob Agents Chemother. (2019) 63(1):e01545-18.

32. Guzel S, Sahinogullari ZU, Canacankatan N, Antmen SE, Kibar D and Coskun Yilmaz B. Potential renoprotective effects of silymarin against vancomycin-induced nephrotoxicity in rats. Drug and chemical toxicology. (2020) 43(6):630-6.

33. Pais GM, Liu J, Zepcan S, Avedissian SN, Rhodes NJ, Downes KJ, Moorthy GS and Scheetz MH. Vancomycin-Induced Kidney Injury: Animal Models of Toxicodynamics, Mechanisms of Injury, Human Translation, and Potential Strategies for Prevention. Pharmacotherapy: The Journal of Human Pharmacology and Drug Therapy. (2020) 40(5):438-54.

34. Ali DA, Abdeen AM, Ismail MF and Mostafa MA. Histological, ultrastructural and immunohistochemical studies on the protective effect of ginger extract against cisplatin-induced nephrotoxicity in male rats. Toxicol Ind Health. (2015) 31(10):869-80.

35. El-Kott AF, Al-Bakry KA and Eltantawy WA. Preventive and curative effects of Zingiber officinale extract against histopathological and Ki-67 immunohistochemical changes of glycerol-induced acute renal failure in rat. Journal of Medical Sciences. (2015) 15(1):25.

36. Baiomy AA and Mansour AA. Genetic and histopathological responses to cadmium toxicity in rabbit's kidney and liver: protection by ginger (Zingiber officinale). Biological trace element research. (2016) 170(2):320-9.

37. Karna P, Chagani S, Gundala SR, Rida PC, Asif G, Sharma V, Gupta MV and Aneja R. Benefits of whole ginger extract in prostate cancer. British journal of nutrition. (2012) 107(4):473-84.

38. Kucukler S, Darendelioğlu E, Caglayan C, Ayna A, Yıldırım S and Kandemir FM. Zingerone attenuates vancomycin-induced hepatotoxicity in rats through regulation of oxidative stress, inflammation and apoptosis. Life Sciences. (2020) 259:118382.

39. Naderi Z, Mozaffari-Khosravi H, Dehghan A, Nadjarzadeh A and Huseini HF. Effect of ginger powder supplementation on nitric oxide and C-reactive protein in elderly knee osteoarthritis patients: A 12-week double-blind randomized placebo-controlled clinical trial. Journal of Traditional and Complementary Medicine. (2016) 6(3):199-203.

40. S Gad S. Effect of ginger as anti-inflammatory agent on serum nitric oxide, tumor necrotic factor α (TNF-α) and interleukin 4 (IL-4) in albino rats with carrageenan induced paw edema. (2018). Msa.edu.eg.

41. Chung HY, Arulkumar R, Bang E, Noh SG and Yokozawa T. Role of Garlic and Ginger in Anti-oxidative and Anti-inflammatory Effects in Aging. SDRP J. Food Sci. Technol. (2019) 4:788-95.

42. Abolaji AO, Ojo M, Afolabi TT, Arowoogun MD, Nwawolor D and Farombi EO. Protective properties of 6-gingerol-rich fraction from Zingiber officinale (Ginger) on chlorpyrifos-induced oxidative damage and inflammation in the brain, ovary and uterus of rats. Chemico-biological interactions. (2017) 270:15-23.

43. Mashhadi NS, Ghiasvand R, Askari G, Hariri M, Darvishi L and Mofid MR. Anti-oxidative and anti-inflammatory effects of ginger in health and physical activity: review of current evidence. International journal of preventive medicine. (2013) 4(Suppl 1):S36.

44. Kafeshani M. Ginger, micro-inflammation and kidney disease. Nutrition. 2015;31:703-7.

45. Bakr AF, Abdelgayed SS, El-Tawil OS and Bakeer AM. Assessment of ginger extract and ginger nanoparticles protective activity against acetaminophen-induced hepatotoxicity and nephrotoxicity in rats. Pakistan Veterinary Journal. (2019) 39:479-86.

46. Abd-Elrhman SY, Abd El-Fattah HM, Morsy GM and Elmasry S. Effect of Ginger Nanoparticles on Hepato-renal Toxicity Induced by Carbon Tetrachloride in Rats. Annual Research & Review in Biology. (2020) :36-55.

47. Zhang M, Xu C, Liu D, Han MK, Wang L and Merlin D. Oral delivery of nanoparticles loaded with ginger active compound, 6-shogaol, attenuates ulcerative colitis and promotes wound healing in a murine model of ulcerative colitis. Journal of Crohn's and Colitis. (2018) 12(2):217-29.

48. Zhuang X, Deng ZB, Mu J, Zhang L, Yan J, Miller D, Feng W, McClain CJ and Zhang HG. Ginger-derived nanoparticles protect against alcohol-induced liver damage. Journal of extracellular vesicles. (2015) 4(1):28713.

الملخص العربى

التأثير الوقائي المحتمل لجسيمات الزنجبيل النانوية المطلية بالكيتوزان مقارنة بالزنجبيل ضد سمية القشرة الكلوية التي يسببها فانكومايسين في الجرذان: دراسة نسيجية وكيميائية مناعية

ايناس رفعت، ايرينى فكرى، سالى سالم محمد، لمياء محمد فرغلى

قسم الأنسجة وبيولوجيا الخلية، كلية الطب، جامعة قناة السويس، مصر

الخلفية والهدف: فانكومايسين هو الخط الأول من المضادات الحيوية في علاج العديد من الالتهابات. تعتبر السمية الكلوية من الآثار الجانبية الأكثر شيوعًا. تم الإبلاغ عن بعض مضادات الأكسدة للتغلب على هذه السمية. تم تسجيل الزنجبيل ليكون أحد هذه العوامل ، علاوة على ذلك ، وجد أن جسيمات الزنجبيل النانوية تتمتع بامتصاص وتوزيع أفضل خاصة عند حملها على حامل نانوي. لذلك ، تم تصميم هذه الدراسة لمقارنة التأثيرات الوقائية المحتملة لجسيمات الزنجبيل النانوية المطلية بالكيتوزان والزنجبيل ضد سمية القشرة الكلوية التي يسببها فانكومايسين في الفئران.

الطريقة: تم اختيار ٦٠ جرذًا بالغًا سليمًا من ذكور الجرذان البيضاء بصورة عشوائية إلى ست مجموعات ، كل منها عشر حيوانات. المجموعة الأولى (التحكم) ، المجموعة الثانية (تم استلام مستخلص الزنجبيل داخل المعدة) ، المجموعة الثالثة (تم تلقي جسيمات الزنجبيل النانوية المغلفة بالشيتوزان داخل المعدة) ، المجموعة الرابعة (تلقيت حقن IP من فانكومايسين) ، المجموعة الخامسة (تلقيت حقنة I.P من فانكومايسين ومستخلص الزنجبيل داخل المعدة) ، المجموعة السادسة (تلقى فانكومايسين وجزيئات الزنجبيل النانوية المغلفة بالشيتوزان داخل المعدة). بعد ٧ أيام تم التضحية بالحيوانات واستخراج الكلى ومعالجة العينات للتقنية النسيجية وتقييم الدرجة النسيجية المتوسطة. تقنيات المناعية الكيميائية وتقييم متوسط الكثافة البصرية للتفاعلات المناعية.

النتائج: أظهرت المجموعة الرابعة أن ٨٠٪ من الحيوانات لديها تغيرات نسيجية مرضية شديدة في الأنابيب الملتفة القريبة مع زيادة معنوية إحصائياً في متوسط الدرجة النسيجية ، مقارنة بمجموعة السيطرة. كان هناك نخر وتقشر في خلاياهم. تم توسيع بعض اللومن الأنبوبي بينما تم إعاقة البعض الآخر بواسطة قوالب من الخلايا المتقشرة. كانت هناك زيادة ذات دلالة إحصائية في متوسط الكثافة البصرية لـ Anti-Caspase ٣ و Anti-iNOS المناعي ، مقارنة بمجموعة التحكم. سجلت المجموعة الخامسة انخفاضاً معنوياً في متوسط الدرجة النسيجية مقارنة بالمجموعة الرابعة ، ولكن زادت معنوياً مقارنة بمجموعة السيطرة. كشفت المجموعة السادسة عن انخفاض كبير في هذه النتيجة ، مقارنة بكل من المجموعة الرابعة والمجموعة السادسة.

الاستنتاج: جسيمات الزنجبيل النانوية المطلية بالكيتوزان ومستخلص الزنجبيل يحسن من سمية القشرة الكلوية التي يسببها الفانكومايسين. ومع ذلك ، أظهرت جزيئات الزنجبيل النانوية نتائج أفضل.